

DTIC FILE COPY

# Interfacial work functions and extrinsic silicon infrared photocathodes

D. D. Coon, R. P. Devaty, A. G. U. Perera, and R. E. Sherriff

Applied Technology Laboratory, Department of Physics, University of Pittsburgh, Pittsburgh, Pennsylvania 15260

(Received 21 June 1989; accepted for publication 22 August 1989)

It is shown that  $n^+$  and/or  $p^+$  contacts on  $p-i-n$  diodes can function as solid-state photoemitters at temperatures  $\lesssim 20$  K. Infrared radiation can excite electrons or holes over small  $n-i$  or  $p-i$  interfacial barriers and into the intrinsic region when the diode is forward biased. Photoelectric thresholds in the far infrared corresponding to 37 and 61  $\mu\text{m}$  cutoffs have been observed for silicon devices using a Fourier transform spectrometer. Suggestions are made to tailor the cutoff wavelengths using different concentrations of various impurities near the metal-insulator transition. Epitaxially grown multilayered (superlattice) detectors are proposed.

AD-A219 748

In this letter, we discuss electronic phenomena at interfaces between heavily doped regions of silicon and undoped regions ( $n-i$  interfaces) in terms of analogies with traditional vacuum tube photocathodes and thermionic cathodes. The relevant energy scale (the interfacial work function) is sufficiently small that low temperatures and low photon energies are required to make the analogies valid.<sup>1</sup> Such analogies can motivate consideration of semiconductor device concepts based on vacuum tube concepts. The device concepts explored here are based on the classic photoelectric effect.<sup>2,3</sup> In addition to regarding  $n-i$  interfaces as photocathodes,  $p-i$  interfaces can be considered to be photoanodes (hole emitters). We suggest that these photocathodes or photoanodes can possess arbitrarily small work functions depending on their impurity concentration and we consider their application to far-infrared detection.

The concept of thermionic emission (thermionic injection) across  $n-i$  interfaces (see Fig. 1) has been described in the work of Yang, Coon, and Shepard.<sup>1</sup> The temperature range (10–30 K) for thermionic emission found in that work was indicative of a low interfacial work function ( $\sim 30$  meV), although this should vary according to the doping concentration and hence the Fermi level in the emitter. The idea is that the Fermi level in an impurity band can lie below the conduction-band edge and account for a work function as indicated in Fig. 1. This idea is also associated with blocked impurity band detectors<sup>4</sup> and other work on extrinsic silicon.<sup>5,6</sup> When the impurity concentration is above the metal-insulator transition, the cathode can be regarded as a metal cathode, otherwise it can be regarded as a semiconductor cathode. The distinction between these two cases hinges on the absence or presence of an impurity band gap separating occupied and unoccupied impurity band states.

In the present work, we operate well below the aforementioned temperature range in order to suppress thermionic emission. Experiments are performed to observe photoelectric thresholds and determine the associated work functions. The concept is to perform experiments which are analogous to classic determinations of work functions of metals.

In the experiments described here, the  $n$  region is Si:P and the  $p$  region is Si:B. The interfaces we utilize are contained in  $p-i-n$  diodes, but the mode of operation of the diodes is radically different from the conventional use of reverse

biased  $p-i-n$  photodiodes for detection of near-infrared, visible, or ultraviolet radiation. The diodes are under forward bias (somewhat in excess of the flatband voltage of about 1.11 eV) and at a temperature of 4.2 K. See Fig. 1. In spite of the forward bias, the diodes fail to pass appreciable current, because the temperature is too low to cause much thermal excitation over the work function barrier shown in Fig. 1. Under these conditions, the dark current at 5 V bias is less than 100 nA ( $< 0.1$  fA) which represents the lower limit of our dc measurement capability. By contrast, currents up to 5 nA are observed under infrared (IR) illumination (high-pressure mercury arc lamp) in the experiment described below. The area of the diode is about 1 mm<sup>2</sup>.

Because of the Fermi level difference between the  $n$ - and  $p$ -contact layers of  $p-i-n$  diodes, photocurrents and thermionic currents are cut off at a bias voltage of  $V < V_0$ . Typically  $V_0 \sim 1.1$  V. This is the flatband voltage as illustrated in Fig. 1. For  $V < V_0$ , electrons and holes are inhibited from entering the  $i$  region. A sharp flatband cutoff in low-temperature data provides a clear indication of interfacial effects. At higher temperatures ( $> 30$  K) the sharpness of the flatband cutoff in current as a function of voltage is degraded.<sup>1</sup>

Spectral information was obtained by Fourier transform spectroscopy using a Specac Michelson interferometer covering the range 50–600  $\text{cm}^{-1}$  (200–16.7  $\mu\text{m}$ ) with a resolution of 16  $\text{cm}^{-1}$ . The interferometer output was phase modulated at 40 Hz and the resulting ac diode current was detected by lock-in amplification. Black polyethylene was

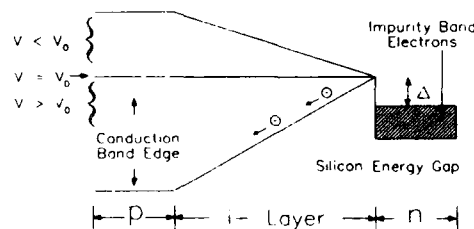


FIG. 1. Illustration of the flatband cutoff, i.e., the effect of bias voltage  $V$  on the injection of carriers from the impurity band into the  $i$  region. Typically,  $V_0 = 1.1$  V. The interfacial work function  $\Delta$  is the offset of the impurity band Fermi level relative to the conduction-band edge in the undoped  $i$  layer. The  $n$  layer (e.g., Si:P) can be regarded as an infrared photocathode. Similarly a  $p$  layer (e.g., Si:B) can be regarded as a photoanode. The sharp triangular barrier at the interface is an idealization which could be approximated using modern epitaxial growth techniques and modulated doping.

used to prevent visible light from reaching the diode.

The low-frequency (long-wavelength) cutoff of the diodes is readily apparent from the spectra as the point where the signal drops to zero (within the noise). This measurement yields a photoelectric threshold of about  $34 \pm 2$  meV ( $37 \pm 2 \mu\text{m}$ ). The high-frequency (short wavelength) cutoff is not obtainable from these spectra since the emission spectrum of the interferometer fades at higher frequencies due to insufficient mirror alignment and decreasing beam splitter effectiveness. The actual shape of the detector spectral response is also not obtainable since the measured spectra are actually convolutions of the detector response, the Specac emission spectrum, and the transmission spectrum of the cold filter used to eliminate background radiation. However, comparisons between the spectral response of different *p-i-n* diodes are possible and a clear difference between photoelectric thresholds is apparent in Figs. 2 and 3.

The temperature must be raised above 4.2 K to produce a measurable dark current. At 16 K the thermionic dark current (Fig. 4) is large enough to clearly display the flatband cutoff. On the other hand, the flatband voltage is not expected to change at the millivolt level between 4.2 and 16 K because the band gap changes by less than a millivolt in this range<sup>7</sup> and Fermi gas estimates of Fermi level shifts indicate that work function changes are similarly small over this temperature range.

The data shown in Fig. 4 are not well described by Fowler cold cathode emission formula.<sup>8,9</sup> Instead, we find that the current *i* (especially for the unfiltered IR response curve) is fairly well described by

$$i = G(V - V_0), \quad (1)$$

where *V* is the bias voltage, *V*<sub>0</sub> is the flatband voltage, and *G* is a temperature and intensity-dependent conductance. The filtered IR response curve in Fig. 4 shows some deviation from the above empirical formula. Since Fig. 4 shows the response to near threshold photons, the results may be associated with the effect of the applied field on threshold. Lowering of the threshold could account for excess current at higher field strengths. A similar effect may influence the thermionic current at 16 K shown in Fig. 4, since an improved fit to low-current data would cause the fit to under-shoot higher current thermionic data. An expression (*eFd*) containing an empirical parameter *d* which describes the lowering of the interfacial work function in an applied field *F* has been given in Ref. 1. Here *e* is the charge of the electron.

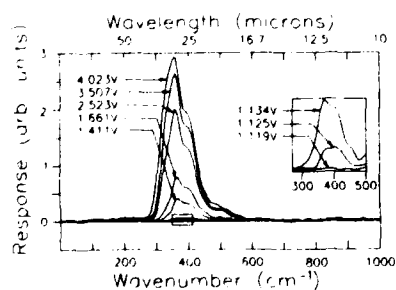


FIG. 2. Response of one *p-i-n* detector for different bias voltages. The cutoff wavelength corresponding to the photoelectric threshold is  $\sim 37 \pm 2 \mu\text{m}$ .

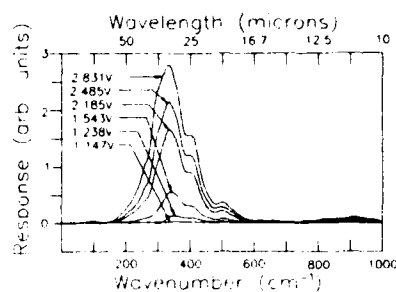


FIG. 3. Response of a second *p-i-n* detector for different bias voltages. The cutoff wavelength corresponding to the photoelectric threshold is about  $61 \pm 2 \mu\text{m}$ .

The data in Figs. 2 and 3 correspond to  $d \approx 0.25$  and  $\approx 0.1 \mu$ , respectively.

Measurement of the spectrum for various detector bias voltages enabled us to find the bias voltage for which the response vanishes. From the bias voltage dependence of the spectral data in Fig. 2, a flatband voltage of  $1.11 \pm 0.01$  V was found using Eq. (1) to extrapolate from a few picoamperes to zero current. This result is in good agreement with the more precise flatband voltage  $1.110 \pm 0.002$  V determined from dc current measurements down to 100 nA and Eq. (1). This provides further support for the photoelectric effect interpretation.

None of the measurements described here permit us to determine whether the photocurrent near threshold is due to electrons or holes. However, the electron and hole work functions  $\Delta_e$  and  $\Delta_h$  can be related to the band gap  $E_{\text{gap}} = 1.170$  eV (Ref. 7) at 4.2 K, and the flatband voltage  $V_0$ . That is,

$$E_{\text{gap}} = eV_0 + \Delta_e + \Delta_h, \quad (2)$$

so that a measurement of  $V_0$  and one work function will permit the other work function to be determined. The cited value of  $E_{\text{gap}}$  includes exciton and phonon corrections. A remarkable fact is that all of the experimentally determined quantities which one would insert in Eq. (2) can be determined to about the same accuracy, i.e., a few meV, although the measurement techniques and issues of interpretation of data are quite different. Spectral measurements reveal the lower of the two work functions. The larger work function is

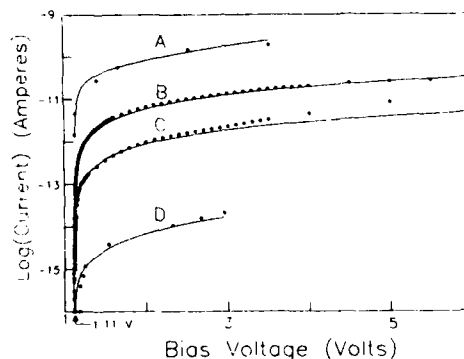


FIG. 4. A—Modulated mercury arc photocurrent with the diode at 4.2 K corresponding to the results in Fig. 3. B—300 K background photocurrent with the diode at 4.2 K. C—Filtered ( $\lambda > 28 \mu\text{m}$ ) 300 K background photocurrent with the diode at 4.2 K. D—Thermionic dark current (diode at 16 K). The dark current at 4.2 K is  $< 10^{-16}$  A. Dots correspond to experimental data points. Lines correspond to fits to Eq. (1).

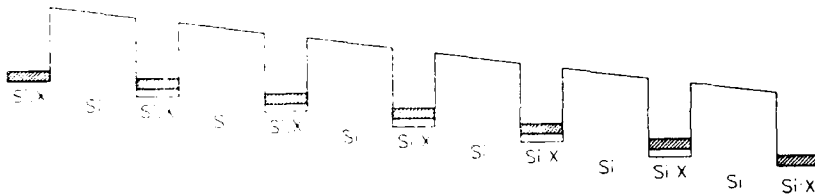


FIG. 5. Proposed multilayered device structure. The doped layer Si:X can be either *p* or *n* type with *X* referring to the dopant.

masked, but it can nevertheless be determined from Eq. (2). An inconsistency will occur if the work function determined by Eq. (2) is lower than the work function determined by spectral measurements. In the case of the diode data shown in Fig. 2, we find that  $\Delta_c \neq \Delta_h$ . Using the band-gap narrowing results of Ref. 6, we estimate that the impurity concentration corresponding to Fig. 2 is about  $4 \times 10^{18} \text{ cm}^{-3}$ , which is near the metal-insulator transition.

Theoretical calculations of Fermi levels in GaAs contact layers<sup>10</sup> adapted to the case of silicon contact layers indicate that as impurity concentrations are increased in the neighborhood of the metal-insulator transition<sup>11,12</sup> ( $3.74 \pm 0.01 \times 10^{18} \text{ cm}^{-3}$  for Si:P), donor impurity band Fermi levels will approach the conduction-band edge and acceptor impurity band Fermi levels will approach the valence-band edge. In other words, the work function  $\Delta$  is a function of the impurity concentration ( $n$ ) with a zero near the metal-insulator transition. Qualitatively similar estimates follow from adapting a formula of Cardona and Ley for work functions of alkali metals.<sup>13</sup> These estimates are imprecise, indicating a need for refinements in theory, but the qualitative feature of  $\Delta(n) = 0$  at an impurity concentration  $n$  near the metal-insulator transition appears to be well founded. Therefore, we expect that interfacial work functions could be made arbitrarily small simply by increasing *n*- or *p*-layer doping. This could provide a wide range of response. For example, one might try to use Si:P cathodes out to wavelengths of about  $130 \mu\text{m}$ , i.e., significantly beyond the expected cutoff of  $27 \mu\text{m}$  [45 meV (Ref. 14)] and to use doped germanium photocathodes well beyond the expected cutoff of  $130 \mu\text{m}$  [9.6 meV (Ref. 14)] for Ge:Sb. This possibility is supported by the preliminary data showing a  $200 \mu\text{m}$  cutoff in a germanium *p-i-n* diode. This idea of extending wavelength cutoffs might also be applied to other impurities. For example, one might consider Si:In devices with response shifted towards the 10–12  $\mu\text{m}$  range or Si:Ga devices with response shifted towards 18–22  $\mu\text{m}$ .

It would be interesting to experimentally explore the dependence of the work function ( $\Delta$ ) on impurity concentration to high precision and to accurately locate a  $\Delta = 0$  concentration relative to the metal-insulator transition. In addition, it would be desirable to utilize abrupt interfaces and uniform impurity concentrations in the *n* and *p* layers, at least in the layer possessing the lowest work function. This would permit detailed theoretical modeling and it would represent an improvement over the present work in which

the *n* and *p* layers are gradually decreasing from a few times  $10^{19} \text{ cm}^{-3}$  in the direction of interface, so that the interface is not precisely defined. This results in a rounded barrier rather than the sharp barrier shown in Fig. 1.<sup>1</sup> Modulation doping in conjunction with epitaxial growth (such as molecular beam epitaxy and chemical vapor deposition<sup>15–18</sup>) appears ideally suited to fabrication of devices with quite uniformly doped layers and very sharp interfaces. In addition, such epitaxial growth techniques would permit the fabrication of multilayered devices as shown in Fig. 5 (e.g., *p-i-p-i...* or *n-i-n-i-n-i...* superlattices) to increase responsivity with *i*-region barriers wide enough to prevent interlayer tunneling in order to achieve low dark currents. The width of *p* or *n* layers would affect response. Relaxation and confinement effects in the doped layers would influence the determination of optimal doped layer widths.

The authors are pleased to acknowledge the efforts of K. M. S. V. Bandara at an early stage of the work. This work was supported in part by the NSF under grant No. ECS-8814664 and the Office of Naval Research under contract No. N00014-85-K-0808.

<sup>1</sup>Y. N. Yang, D. D. Coon, and P. F. Shepard, *Appl. Phys. Lett.* **45**, 752 (1984).

<sup>2</sup>P. Lenard, *Ann. Physik* **2**, 359 (1900).

<sup>3</sup>A. Einstein, *Ann. Physik* **17**, 132 (1905).

<sup>4</sup>M. D. Petroff, M. G. Stapelbroek, and W. A. Kleinhaus, *Appl. Phys. Lett.* **51**, 406 (1987).

<sup>5</sup>A. Miller and E. Abrahams, *Phys. Rev.* **120**, 745 (1960).

<sup>6</sup>J. Wagner and J. A. del Alamo, *J. Appl. Phys.* **63**, 425 (1988).

<sup>7</sup>W. Bludau, A. Onton, and W. Heinke, *J. Appl. Phys.* **45**, 1846 (1974).

<sup>8</sup>R. H. Fowler and L. Nordheim, *R. Soc. Proc. A* **119**, 173 (1928).

<sup>9</sup>L. W. Nordheim, *R. Soc. Proc. A* **121**, 628 (1928).

<sup>10</sup>K. M. S. V. Bandara and D. D. Coon, *Superlatt. Microstruct.* **4**, 705 (1988).

<sup>11</sup>N. F. Mott, *Metal-Insulator Transitions* (Barnes and Noble, New York, 1974).

<sup>12</sup>T. F. Rosenbaum, R. F. Milligan, M. A. Paalanen, G. A. Thomas, and R. N. Bhatt, *Phys. Rev. B* **27**, 7509 (1983).

<sup>13</sup>M. Cardona and L. Ley, Introduction in *Topics in Applied Physics, Vol 26: Photoemission in Solids I*, edited by M. Cardona and L. Ley (Springer, New York, 1978).

<sup>14</sup>S. M. Sze, *Physics of Semiconductor Devices* 2nd edition (Wiley, New York, 1981), p. 21.

<sup>15</sup>G. H. Dohler, H. Kunzel, D. Olego, K. Ploog, P. Ruden, H. J. Stolz, and G. Abstreiter, *Phys. Rev. Lett.* **47**, 864 (1981).

<sup>16</sup>M. Hundhausen, L. Ley, and R. Carius, *Phys. Rev. Lett.* **53**, 1598 (1984).

<sup>17</sup>D. H. Zang and D. Haneman, *Appl. Phys. Lett.* **52**, 1392 (1988).

<sup>18</sup>M. W. Denhoff, T. E. Jackman, J. P. McCaffrey, J. A. Jackman, W. N. Lennard, and G. Massoumi, *Appl. Phys. Lett.* **54**, 1332 (1989).

SEARCHED  INDEXED

SERIALIZED  FILED

Dist Special

A-1 21

Coon et al. 1740